ORIGINAL ARTICLE

How Host Population Dynamics Translate into Time-Lagged Prevalence: An Investigation of Sin Nombre Virus in Deer Mice

Frederick R. Adler[a,*], Jessica M.C. Pearce-Duvet[b], M. Denise Dearing[b]

[a] Department of Mathematics and Department of Biology, 155 South 1400 East, University of Utah, Salt Lake City, UT 84112, USA
[b] Department of Biology, 257 South 1400 East, University of Utah, Salt Lake City, UT 84112, USA

Abstract Human cases of hantavirus pulmonary syndrome caused by Sin Nombre virus are the endpoint of complex ecological cascade from weather conditions, population dynamics of deer mice, to prevalence of SNV in deer mice. Using population trajectories from the literature and mathematical modeling, we analyze the time lag between deer mouse population peaks and peaks in SNV antibody prevalence in deer mice. Because the virus is not transmitted vertically, rapid population growth can lead initially to reduced prevalence, but the resulting higher population size may later increase contact rates and generate increased prevalence. Incorporating these factors, the predicted time lag ranges from 0 to 18 months, and takes on larger values when host population size varies with a longer period or higher amplitude, when mean prevalence is low and when transmission is frequency-dependent. Population size variation due to variation in birth rates rather than death rates also increases the lag. Predicting future human outbreaks of hantavirus pulmonary syndrome may require taking these effects into account.

1. Introduction

The 1993–1994 outbreak of hantavirus pulmonary syndrome (HPS) in humans in the American southwest was caused by Sin Nombre virus (SNV), and was quickly correlated with the high rainfall associated with the large El Nino (ENSO) event of the previous year that led to the increased populations of deer mice (*Peromyscus maniculatus*), the primary host of the virus (Schmaljohn and Hjelle, 1997; Engelthaler et al., 1999). However, further study has shown that the link between weather and HPS

---

cases is quite complex (Glass et al., 2000), involving at best a noisy trophic cascade from weather, plants, deer mouse population size, and deer mouse infection prevalence before humans are finally affected (Engelthaler et al., 1999; Mills et al., 1999; Yates et al., 2002; Kolivras and Comrie, 2004). The magnitude and timing of the response at each step depends on the detailed behavior of individual species: the many species of plants, the feeding and reproduction of deer mice, the transmission dynamics of the virus between deer mice, and the transmission to humans. The ecological steps, from rain to rodents, have proven to be quite unpredictable (Brown and Ernest, 2002). Indeed, there is debate about whether the 1997 ENSO event led to an increase in HPS cases beginning in the spring of 1998 (Hjelle and Glass, 2000; Kolivras and Comrie, 2004).

Although frequently fatal to humans, the effects of SNV on deer mice are nonexistent or weak (Helle and Yates, 2001), although there is evidence of higher mortality in subadults (Douglass et al., 2001). Deer mice apparently remain seropositive throughout life, and the infection can be modeled as if there is no recovery (Mills et al., 1999; Kuenzi et al., 2005), although antibody loss may be possible (Boone et al., 1998). Transmission is primarily through biting (Botten et al., 2002), although there is evidence of oral/fecal transmission in burrows (Mills et al., 1999), with no vertical transmission from parents to offspring. Prevalence of infection is generally higher in males and in older individuals, and large older males are particularly likely to carry the infection (Boone et al., 1998; Abbott et al., 1999).

In diseases without vertical transmission, population dynamics can have two conflicting effects on prevalence (Mills et al., 1999). During periods of rapid population growth, the lack of vertical transmission leads to dilution and potentially reduced prevalence. However, the resulting higher population size is likely to increase contact rates between deer mice that could eventually lead to an increase in prevalence.

These conflicting effects have appeared in the literature as inconsistent results regarding the link between population size and SNV seroprevalence (Table 1). Only a few studies have found a positive relationship between current population size and seroprevalence, and others have found a positive relationship only in the presence of a lag (Davis et al., 2005). In the system under consideration in this paper, several studies have found no linear relationship between current population size and prevalence (Graham and Chomel, 1997; Mills et al., 1997; Boone et al., 1998), and our reanalysis of data presented in two other papers shows the same result (Calisher et al., 1999; Root et al., 1999). There is evidence for a threshold effect in that sufficiently small populations showed a prevalence of zero (Boone et al., 1998). Negative correlations were found in two out of ten time series of SNV seroprevalence versus population size in Montana (Douglass et al., 2001). Using multivariate analysis, one study found a positive effect of deer mouse density on prevalence (Biggs et al., 2000).

Studies of other hantaviruses have found similarly inconsistent results. In the closely related Limestone Canyon virus (Sanchez et al., 2001), higher prevalence was observed during periods of low population density (Abbott et al., 1999), consistent with a negative correlation. A recent study found a negative correlation between density and prevalence in El Moro Canyon virus in western harvest mice (Calisher et al., 2005). In bank voles, Puumala virus seroprevalence was well predicted in part by the phase of population, being highest after the peak, implying both density-dependence and delayed density-dependence (Olsson et al., 2002, 2003).

Table 1 Correlation between current density and prevalence

Mean prevalence (%)	Relationship[a]	Reference
9.5	0	(Calisher et al., 1999)
11.0	0	(Mills et al., 1997)
11.9	−	(Calisher et al., 2005)
14.3	0	(Root et al., 1999)
15.8	−	(Douglass et al., 2001)
16.5	+	(Biggs et al., 2000)
17.0	0	(Graham and Chomel, 1997)
17.8	−	(Abbott et al., 1999)
18.5	0	(Boone et al., 1998)

[a]+ indicates a significant positive relationship, − a significant negative relationship, and 0 the lack of a significant relationship

In plague, another disease of rodents, one study found that a model with a two year delay performed well in predicting presence or absence of disease as a function of the proportion of burrows occupied by great gerbils (Davis et al., 2004). Frequency of human plague cases increased with a one or two year lag as a function of winter or summer precipitation (Enscore et al., 2002), although this could be due to a direct numbers effect rather than increases in seroprevalence.

The interplay between dilution due to births and increased prevalence due to higher contact rates depends sensitively on how contact rates vary with host density. Models range from a constant contact or frequency-dependent model, where the contact rate is independent of population size and the force of infection is proportional to the frequency of infected hosts, to a mass action or density-dependent model, where the contact rate is proportional to population size and the force of infection is proportional to the number of infected hosts (McCallum et al., 2001). Intermediate models, where the contact rate saturates as host density becomes large, can result from behavioral changes at low density (Ramsey et al., 2002) or from host heterogeneity (Barlow, 2000). Such models can produce substantially different predictions about disease dynamics and persistence, and may be distinguishable with field data (Caley and Ramsey, 2001). The contact rate depends on the territorial behavior of hosts (Wolff, 1985). As density increases from low levels, deer mice decrease home range size, thus potentially leaving contact rates unchanged. As density increases further, deer mice increase aggression and perhaps effective contact rates without further decrease in home range size.

Mathematical models of the temporal dynamics of hantaviruses have yet to explicitly consider lags. The models have focused instead on spatial spread and the role of refugia for the virus when population sizes are small (Abramson and Kenkre, 2002). Further analysis showed that seasonality can promote disease persistence and cause outbreaks (Buceta et al., 2004). In particular, the maximum infected population occurs near the end of the harsh season, and thus substantially delayed from the period of optimal reproduction. A recent paper shows that human outbreaks can be induced by population size increases in rodents that quickly generate many highly infectious new infections (Sauvage et al., 2007).

This paper identifies a simple epidemiological model that can capture the major trends in prevalence, and uses that model to study the relationship between population size and

prevalence. The key parameters are birth, death, and transmission rates, which we hypothesize create characteristic time lags between population size and prevalence. We begin by fitting published data (Yates et al., 2002) with a simple model, and illustrate the sensitivity of the results to the model parameters, particularly those describing transmission. We then use this simple model to show that the lag has a complex relationship with population dynamics which depends on the details of the transmission process in addition to host demographic parameters.

2. Model and parameter estimates

Our model is an SI model of susceptible and infected individuals (Anderson and May, 1992)

$$\frac{dS}{dt} = -cg(N)pS + bN - \delta S,$$

$$\frac{dI}{dt} = cg(N)pS - \delta I,$$

where S, I and N represent the density of susceptible, infected, and total hosts, respectively, and $p = \frac{I}{N}$ is the prevalence. The parameter c describes the effective contact rate per day, and b and δ give the birth and death rates, respectively, and can be functions of time. Table 2 gives a complete description of the parameters in the model and their baseline values.

The function $g(N)$ describes the dependence of contact rate on density. We chose a variant of asymptotic transmission (McCallum et al., 2001) with the form

$$g(N) = \left(\frac{N_d + K}{N_d}\right)\left(\frac{N}{N + K}\right). \tag{1}$$

Here K gives the density where contact is 50% of maximum, and N_d is a scaling factor equal to the density where $g(N) = 1$. If $K = 0$, $g(N) = 1$ for all N, corresponding to a model with constant contact rates and frequency-dependent transmission. As $K \to \infty$,

Table 2 Variables and parameters in the model

Symbol	Description	Baseline value
N	Density of deer mice	
I	Density of infected deer mice	
S	Density of susceptible deer mice	
p	Prevalence of infection	
δ	Mortality rate per day	0.01
b	Birth rate per day (after natal mortality)	0.02
c	Effective contact rate per day	0.0105 with variation in births
		0.022 with variation in deaths
$g(N)$	Dependence of contact rate on density	$g(N) = \left(\frac{N_d + K}{N_d}\right)\left(\frac{N}{N + K}\right)$
K	Density where contact is 50% of maximum	50 mice/ha
N_d	Density where $g(N) = 1$	7 mice/ha

$g(N) \to N/N_d$, corresponding to a mass action model and density-dependent transmission.

The equations can be rewritten in terms of the prevalence p and total density N as

$$\frac{dp}{dt} = cg(N)p(1-p) - bp, \tag{2}$$

$$\frac{dN}{dt} = bN - \delta N. \tag{3}$$

Mortality does not differ between susceptible and infected deer mice and thus plays no direct role in the equation for prevalence. A higher birth rate b reduces prevalence because there is no vertical transmission. If contact rates increase with increasing population size, a higher birth rate will lead to increased population size and a delayed increase in prevalence. The disease will persist in an isolated population with constant coefficients if the average effective contact rate $cg(N)$ exceeds the average of the birth rate b.

Our parameter estimates for the baseline birth and death rates come from studies that deduce death rates from population change during the nonbreeding winter season (roughly $\delta \approx 0.008$) and birth rates from the growth during the breeding season ($r = b - \delta \approx 0.007$) (Petticrew and Sadleir, 1974; Fairbairn, 1977). The baseline value of K was chosen based on the assumption that mouse behavior changes at densities of over 30 deer mice per hectare (Wolff, 1985). The scaling factor N_d is the mean density found in Yates et al. (2002). The transmission rates c were found by matching the observed mean prevalence in Yates et al. (2002). With a large value of K, our model approximates "pseudo mass action model" in a study of cowpox in bank voles (Begon et al., 1998), which found, in the units of the current work, c in the range from 0.006 to 0.008, slightly lower than our estimates.
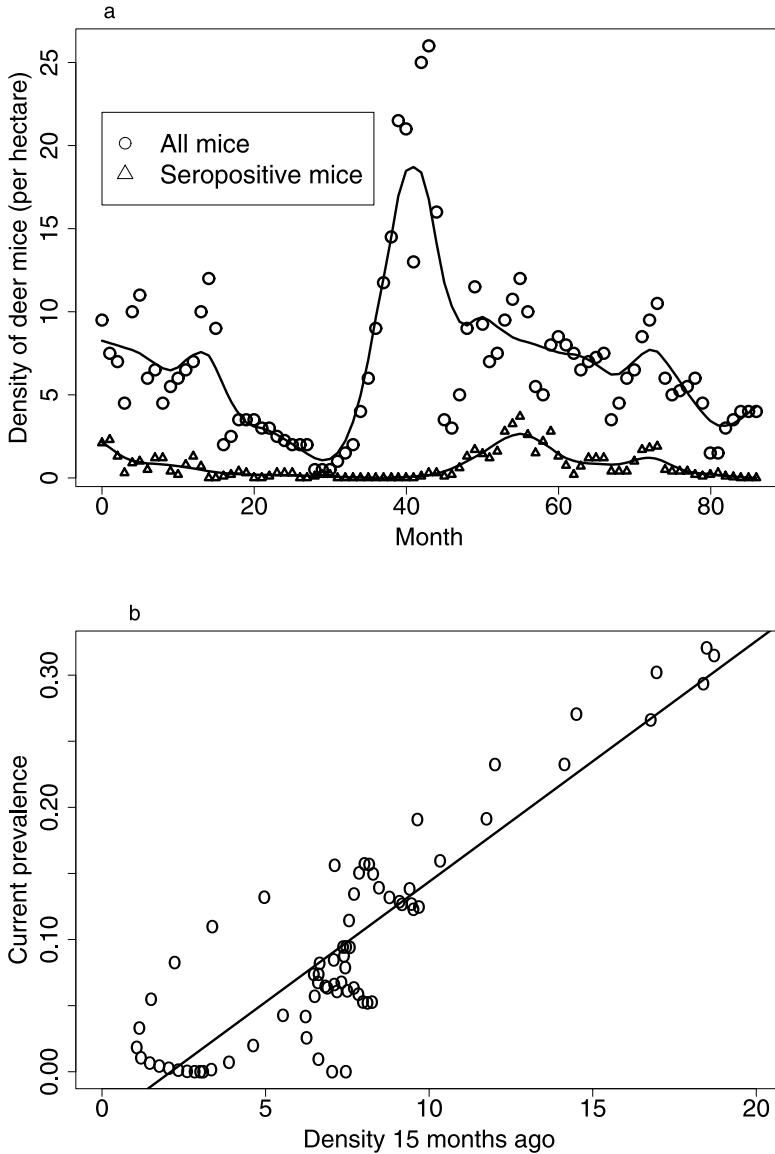
3. Comparing the model with data

We extracted data on the density of deer mice and of seropositive deer mice from Yates et al. (2002), and show the raw data and smoothed data over an 87 month period (created with the supsmu function in R (R Development Core Team, 2005)) in Fig. 1a. We use smoothed data in the following analyses to average over factors creating noise in the original data and to interpolate values for missing data points.

We examined the correlations between prevalence and lagged population size. We found the strongest correlation with population size 15 months earlier, although there was significant correlation with a lag of 12 months as found by Yates and others (Fig. 1b).

Using the time series for the density of all mice, we computed the growth rate $r = b - \delta$ as a function of time that exactly matches the smoothed density trajectory. We created two versions of our model:

- *Variable birth rates*: Set the death rate $\delta(t)$ to be constant and solve for the birth rate $b(t)$ as a function of time.
- *Variable death rates*: Set the birth rate $b(t)$ to be constant and solve for the death rate $\delta(t)$ as a function of time.

Fig. 1 (a) Comparison of raw data and smoothed data from Yates et al. (2002) showing the density of deer mice and of seropositive deer mice over an 87 month period. (b) Plot of prevalence against density with the optimal lag of 15 months, chosen as the lag that maximizes r^2.

This fit does not use any information about seroprevalence. With our baseline parameter values, the model predicts the dynamics of the infection reasonably well (Fig. 2). The model with varying death rates requires a larger value of the contact rate c because our baseline birth rate is higher than the baseline death rate (Fig. 2b).
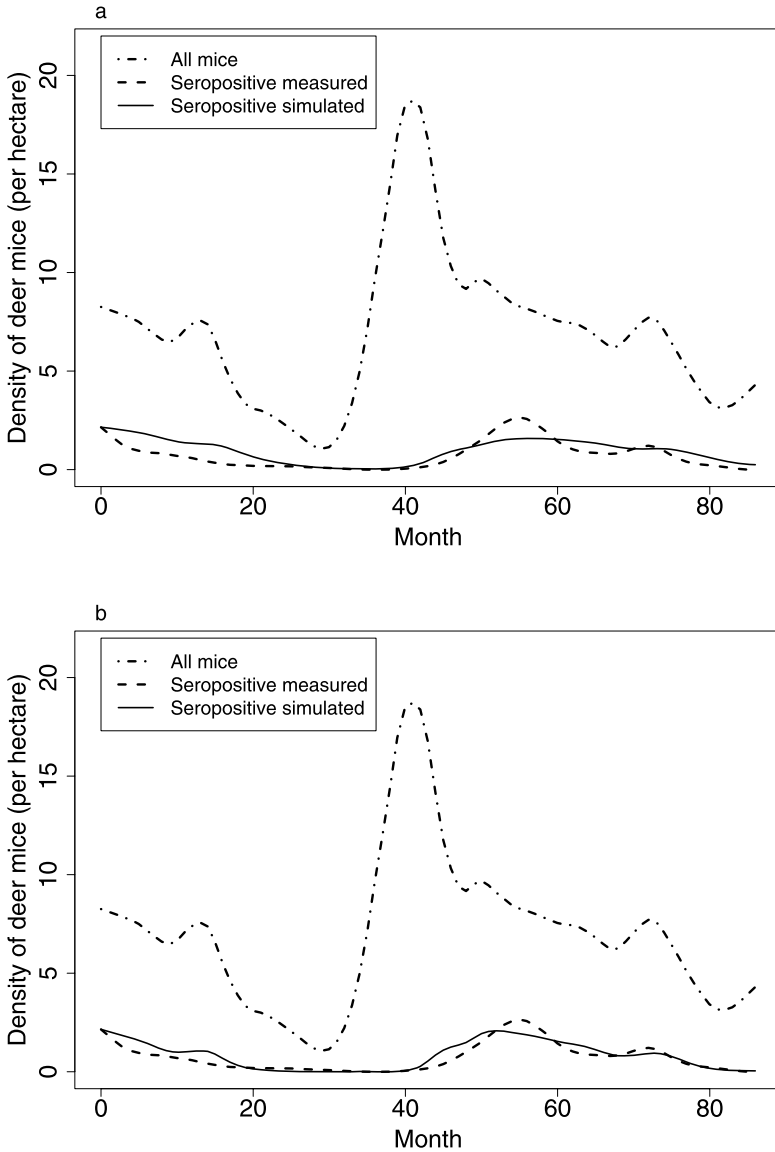
Fig. 2 Modeled density of seropositive mice with (a) variable birth rates, and (b) variable death rates. The modeled density of all mice is set to exactly match the smoothed data. Parameter values as in Table 2.

The two cases make slightly different predictions about the correlations with lagged population size and growth rate. The model with variable birth rates matches the observed lag somewhat better (Fig. 3) but has lower r^2 values. It generates a significant positive correlation when the lag is at least 6 months, and a significant negative correlation when
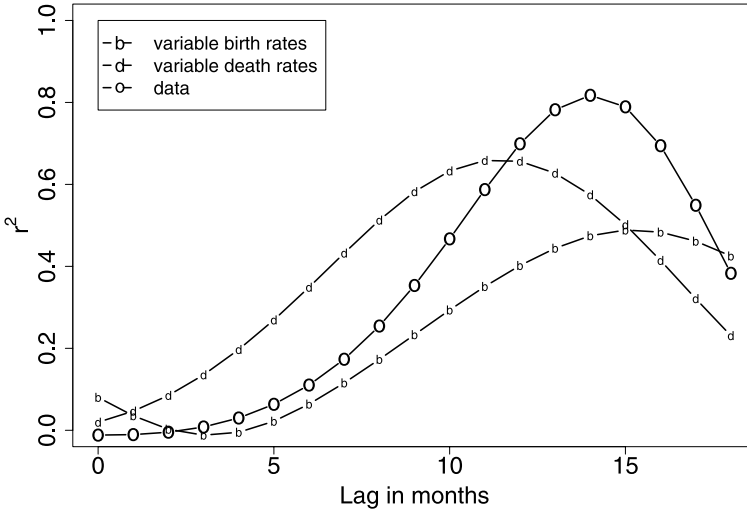
Fig. 3 The coefficient of determination r^2 of prevalence as a function of lagged density for a range of lags for the actual data (open circles), and the two simulations shown in Fig. 2 (b's with variable birth rates, d's with variable death rates).

the lag is 0 or 1 month. The model with variable death rates generates a significant positive correlation when the lag is at least 2 months.

The model results are extremely sensitive to the choice of the contact rate c. Small increases or decreases lead not only to large changes in the number of infected individuals, but also to changes in the lag between peaks of population density and of seropositivity, with higher contact rates generating a substantially shorter lag (Fig. 4).

4. Theory: lags induced by oscillating population size

What aspects of the data produce the observed lags? In this section, we use linear perturbation theory to calculate the lags induced by sinusoidal population oscillations with different periods, and then use Fourier analysis to decompose the observed population size data into a sum of sinusoidal oscillations to identify key aspects of the data.

4.1. Linear perturbation theory

As described in detail in the Appendix, we assume that the population size $N(t)$ varies in a small amplitude sinusoidal oscillation around a mean value of N_0, or

$$N(t) = N_0 + \epsilon \alpha \cos(2\pi \omega t).$$

Here, ϵ is a small parameter, α scales the magnitude of the oscillation, and ω is the frequency of the oscillation. Using the equation for population size (Eq. (3)), we can compute the small amplitude sinusoidal oscillation describing the birth or death rate, depending on the case under consideration.
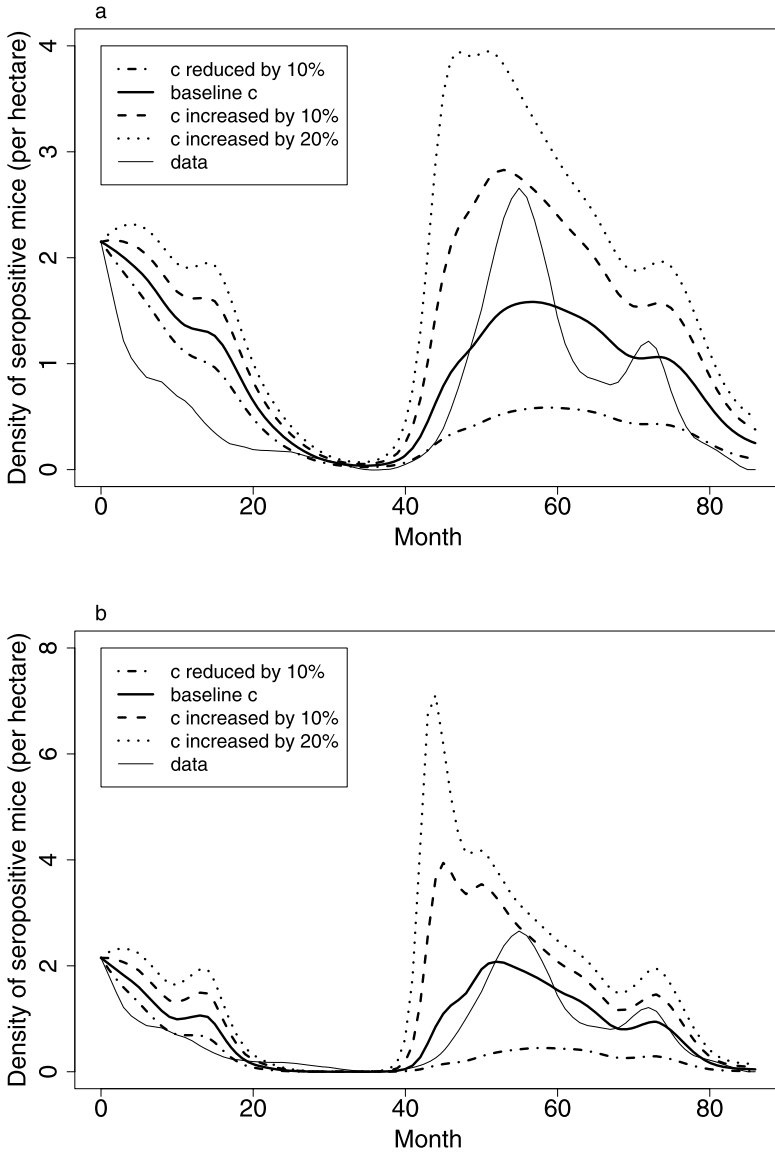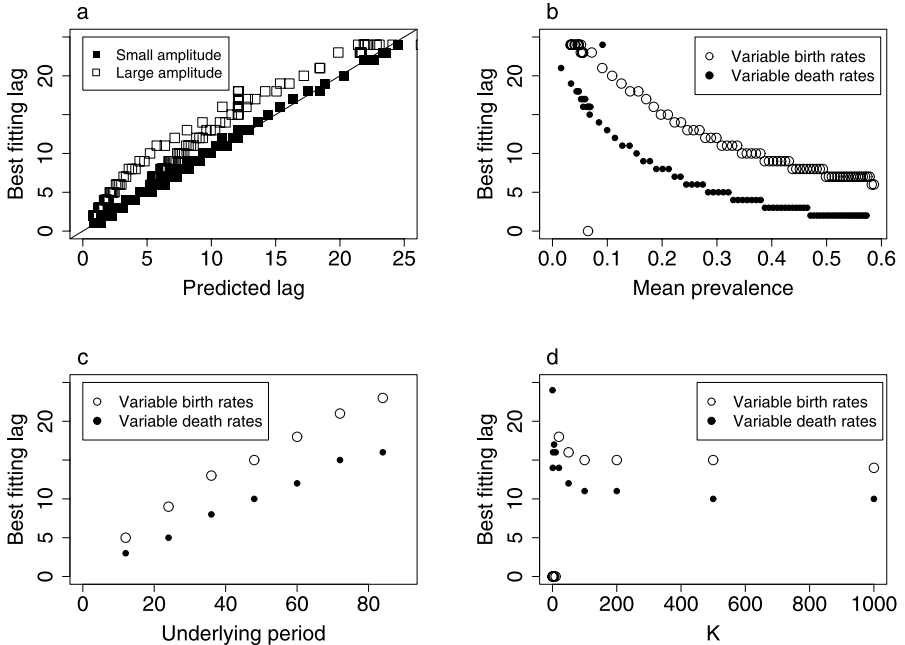
Fig. 4 Effects of changing the contact rate *c* on the dynamics of seroprevalence with (a) variable birth rates, and (b) variable death rates. Parameter values as in Table 2.

Substituting these oscillations into the basic equation for prevalence (Eq. (2)), we can write

$$p(t) = p^* + \epsilon Z \cos\big(2\pi \omega (t - \phi)\big),$$

Fig. 5 (a) Comparison of computed lags from the linear theory with the statistically estimated lags from simulations. Solid squares show simulations with $\alpha = 1$, a low amplitude oscillation, and open squares simulations with $\alpha = 4$, an amplitude comparable to that in the real data. The statistically estimated lags are those giving the highest r^2 value. Parameters were varied separately around the baseline values in Table 2, with c running from 0.01 to 0.03 in the case with variable birth rates and from 0.02 to 0.06 in the case with variable birth rates and K running from 0 to 1024. The underlying period is 87 months throughout. All simulations were run for 240 months. (b) The effect of mean prevalence on the observed lag, using the parameter values in Table 2 with $\alpha = 4$ and an underlying period of 87 months throughout. Open circles show the case with variable birth rates, and solid circles show the case with variable death rates. (c) The effect of period on the observed lag, using periods in multiples of 12 months from 12 to 84. Other parameters as in Table 2. (d) The effect of K on lags using the parameter values in Table 2 and an underlying oscillation with amplitude 4 and period 87 months, but adjusting c to match the mean prevalence observed in the data.

where p^* is the mean prevalence, Z is the scaled amplitude, and ϕ is the phase shift or lag induced by the dynamics. We can use methods from perturbation theory to solve explicitly for Z and ϕ in terms of the parameter values.

Figure 5a shows that the exact lag from the linear theory compares well with the statistical fits to the simulation, and that higher amplitude oscillations (of a similar magnitude to those observed) produce longer lags than small amplitude oscillations. Much of the variation in lags for a fixed period of the population size oscillation is generated by two factors (Fig. 5b). Higher mean prevalence produces substantially shorter lags as does attributing the variation in population size to variation in the death rate. The observed lag does not vary linearly with the period of the population size oscillation, but eventually saturates to a fixed value that depends on the other parameters (Fig. 5c). If we control for the mean prevalence by adjusting c, larger values of K lead to shorter lags with substan-
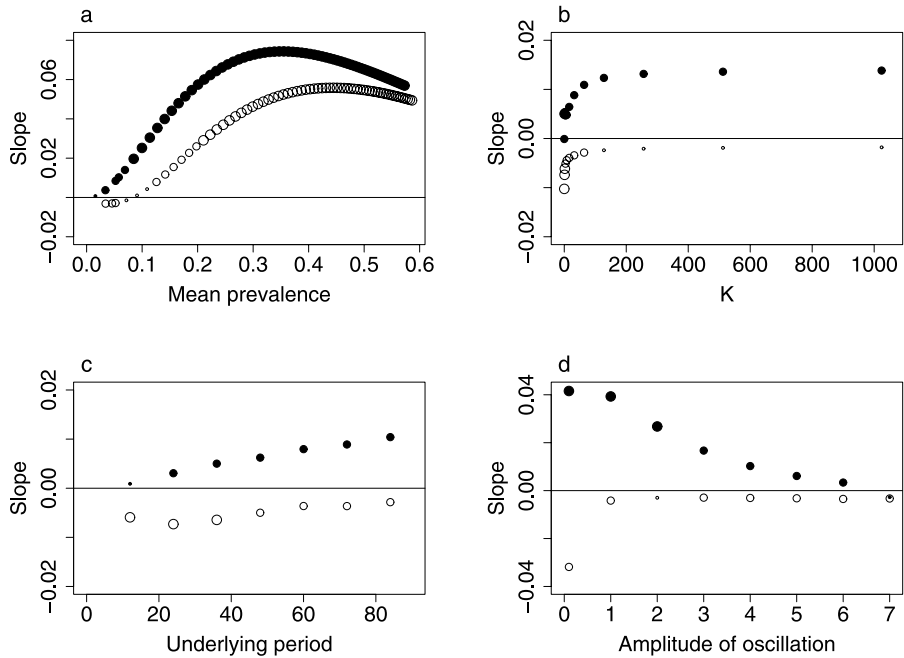
Fig. 6 The slope of the relationship between current density and prevalence, open circles show the case with variable birth rates, and solid circles show the case with variable death rates. Large circles show cases with a statistically significant relationship ($p < 0.05$) and $r^2 > 0.2$, slightly smaller circles show cases with a statistically significant relationship and $r^2 <= 0.2$, and small circles show cases with an insignificant relationship. (a) The effect of mean prevalence, using the range of parameters from Fig. 5a. (b) The effect of K, after controlling for mean prevalence as in Fig. 5d. (c) The effect of the underlying period on r^2 over the range of parameters used in Fig. 5c. (d) The effect of the amplitude of the density oscillation. The data have an amplitude of about 4.0.

tially higher r^2 values, except that small values of K and variation in birth rates leads to a lag of zero (Fig. 5d).

Using the same range of parameter values, we can check for a significant correlation between prevalence and population size in the absence of a lag by regressing $p(t)$ against $N(t)$. Both the significance and slope of the relationship are generally lower with low prevalence, and low prevalence in combination with variation in birth rates produces a significant negative relationship (Fig. 6a). Smaller values of K, and thus frequency-dependent transmission, have a lower value of the slope (Fig. 6b). With variation in death rates, we observe a stronger positive relationship when the underlying period is large (Fig. 6c). With variation in birth rates, we observe a stronger negative relationship when the underlying period is small (Fig. 6c). Finally, the strength of the relationship is weaker when the amplitude of the oscillation is large (Fig. 6d).

4.2. Fourier analysis

We used Fourier analysis to determine the underlying periods in the smoothed population data from Yates et al. (2002). The dominant modes are the longer periods, and much of
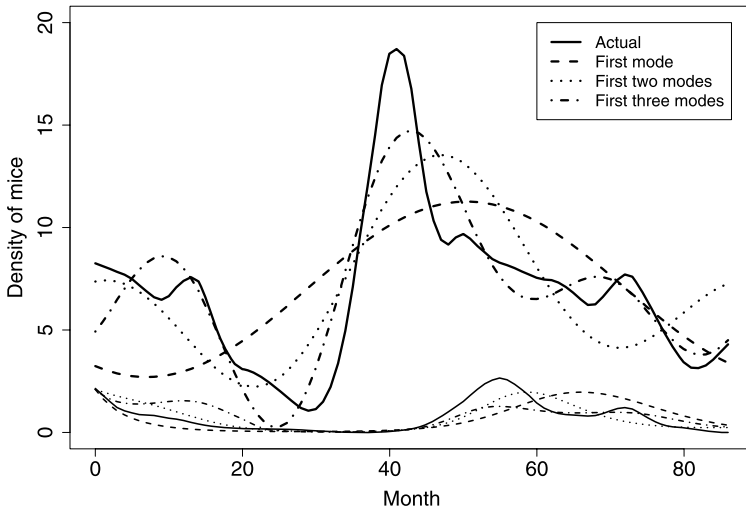
Fig. 7 The effect of including more Fourier modes in the approximation of the density dynamics.

the pattern of variation is captured by the first three modes (with periods of 87 months, $\frac{87}{2}$ months, and $\frac{87}{3}$ months) (Fig. 7). However, the predicted lag is decreased by the higher modes, taking on a value of 22 months with only the lowest mode, and a value of 16 months when the higher modes are included. The observed lag thus results not only from the fact that the data have a single peak, and are thus fit by a single sinusoidal oscillation, but also to the nonsinusoidal shape of the population size trajectory.

5. Discussion

The time lag between population size and prevalence in horizontally transmitted diseases is determined by the interplay between dilution, the reduced prevalence caused by periods of rapid population growth in the absence of vertical transmission, and increased transmission at higher density. A simple model tracks prevalence as a function of population size, and derives host birth and death rates from the population trajectory itself in two ways: assigning all variation to the birth rate while keeping the death rate constant, or assigning all variation to the death rate while keeping the birth rate constant. When the host population follows a small amplitude sinusoidal oscillation, we can analytically calculate the lag between population size and prevalence.

We find that the lag is not a simple function of the host demographic parameters, but is sensitive to the details of host population size variation, the mean prevalence, and the assignment of variation to host birth or death rates. Significant lags using reasonable parameter values range from 0 to 18 months, with longer lags associated with larger amplitude population oscillations (Fig. 5a), lower prevalence (Fig. 5b), longer underlying periods (Fig. 5c), and frequency-dependent transmission (Fig. 5d). Assignment of host population variation to changes in birth rates also increases the duration of the lag. This effect

is not due to differences in total population size (which is matched to the observed population size in each case), but rather to the differences in age structure, with many young uninfected mice appearing during periods of growth. These lags often greatly exceed the lifespan of individual hosts, resulting from the slow increase or decrease in prevalence in the whole population.

A simple model provides a reasonably good quantitative fit to published data (Yates et al., 2002), but is highly sensitive to the contact rate parameter (Fig. 4). Using Fourier analysis to decompose the data into a sum of sinusoidal oscillations captures the main trends, but the subtler details of the population trajectory affect the observed lag (Fig. 7).

Although the optimal lag is rarely zero, there is often a significant correlation between current density and prevalence in a given time series. However, with variation in birth rates, the relationship is predicted to switch from negative to positive when the prevalence increases through about 10%. Interestingly, the prevalences reported in studies that looked for such correlations lie in this range (Table 1). Given the many differences in study site and study system, it is less than surprising that there is no trend among these observed values.

Our simple model neglects many factors known to be important in the dynamics of SNV. Males typically have higher prevalence and presumably higher effective contact rates (Allen et al., 2006). Age and size also play important roles, with older rodents sometimes proving crucial to the persistence of the disease (Calisher et al., 2001), and larger males having higher prevalence (Boone et al., 1998; Abbott et al., 1999). Alternative mechanisms of transmission, through the environment (Sauvage et al., 2003) or through other reservoir species (Keesing et al., 2006) can have major damping effects of the dynamics of prevalence. Finally, some evidence indicates that infectiousness changes with time since infection (Botten et al., 2002; Kuenzi et al., 2005). Given the extreme sensitivity of the results to the contact rate, this complication warrants further investigation.

Spatial effects are likely to be important in several ways. First, movement of infected animals is common (Root et al., 2003), with one study showing that mobile animals typically have higher prevalence (Escutenaire et al., 2000). Second, the disease may persist in spatial refugia during periods of low population and prevalence (Mills et al., 1999), and recolonize from those regions during periods of population increase, leading to longer lags (Abramson and Kenkre, 2002). Finally, small scale variation in weather and habitat can lead to desynchronized dynamics over small spatial scales, and movement can lead to complex patterns (Engelthaler et al., 1999; Glass et al., 2000).

A full appreciation of the dynamics of hantavirus in wild populations of mice will almost certainly require longer time series of higher resolution data, including information on sex, age and size of the individuals sampled, on the seroprevalence of and contact rates with alternative reservoir species, and on the environmental covariates known to be important in altering dynamics. Whether such detailed information will enable us to more accurately predict future outbreaks of hantavirus infections in humans remains to be seen.

Appendix A

Consider the basic model for prevalence given by Eq. (2),

$$\frac{dp}{dt} = cg(N)p(1-p) - bp$$

and assume that

$$N(t) = N_0 + \epsilon n(t)$$

for some small parameter ϵ. From Eq. (3), we have that

$$\frac{dN}{dt} = \big(b(t) - \delta(t)\big)N.$$

Assume that

$$b(t) = b_0 + \epsilon x(t),$$
$$\delta(t) = b_0 + \epsilon w(t).$$

We have set the mean birth and death rates equal in order to maintain a constant average population size. Then the per capita reproduction is

$$\frac{\frac{dN}{dt}}{N} = \frac{\epsilon n'(t)}{N_0 + \epsilon n(t)} = b(t) - \delta(t).$$

We examine two cases, as in the analysis of the data. With a variable birth rate $b(t)$ and a constant death rate $\delta(t)$,

$$x(t) = \frac{n'(t)}{N_0 + \epsilon n(t)} \approx \frac{n'(t)}{N_0}, \tag{A.1}$$

$$w(t) = 0 \tag{A.2}$$

by neglecting higher order terms in ϵ. With a variable death rate $\delta(t)$ and a constant death rate $b(t)$,

$$x(t) = 0, \tag{A.3}$$

$$w(t) = \frac{-n'(t)}{N_0 + \epsilon n(t)} \approx \frac{-n'(t)}{N_0}. \tag{A.4}$$

We can use these expansions to expand $p(t)$ around its stable equilibrium p^* when $\epsilon = 0$, where

$$p^* = \begin{cases} 1 - \frac{b_0}{cg(N_0)} & \text{if } cg(N_0) \geq b_0, \\ 0 & \text{if } cg(N_0) < b_0. \end{cases} \tag{A.5}$$

Assuming $p^* > 0$, set

$$p(t) = p^* + \epsilon z(t).$$

Expanding and retaining only terms of order ϵ gives

$$\frac{dz}{dt} = \big(cg'(N_0)p^*(1 - p^*)n(t) - x(t)p^*\big) + \big(cg(N_0)(1 - 2p^*) - b_0\big)z(t). \tag{A.6}$$

Now assume that $n(t)$ is an oscillation with amplitude α and period $T = \frac{1}{\omega}$, or

$$n(t) = \alpha \cos(2\pi \omega t).$$

Then

$$\frac{dz}{dt} = A \cos(2\pi \omega t) + B \sin(2\pi \omega t) + Cz(t), \tag{A.7}$$

where

$$
\begin{aligned}
A &= \alpha c g'(N_0) p^* (1 - p^*), \\
B &= \begin{cases} \frac{2\pi \omega \alpha p^*}{N_0} & \text{with variable birth rates,} \\ 0 & \text{with variable death rates,} \end{cases} \\
C &= c g(N_0)(1 - 2p^*) - b_0.
\end{aligned}
\tag{A.8}
$$

Assuming p^* is positive, and that the disease can persist, we can use Eq. (A.5) to substitute for p^* and rewrite the coefficient C as

$$C = -c g(N_0) p^* < 0.$$

Equation (A.7) is linear and can be solved explicitly as

$$z(t) = K e^{Ct} + \frac{(2A\pi \omega - BC) \sin(2\pi \omega t) - (AC + 2B\pi \omega) \cos(2\pi \omega t)}{C^2 + (2\pi \omega)^2}. \tag{A.9}$$

The exponential term decays to zero because $C < 0$. To find the lag ϕ and the amplitude Z induced by the dynamics, we write the oscillatory part as

$$z(t) = Z \cos\big(2\pi \omega (t - \phi)\big).$$

We can solve for Z and ϕ as

$$Z = \sqrt{\frac{A^2 + B^2}{C^2 + (2\pi \omega)^2}},$$

$$\phi = \frac{\tan^{-1}\left(\frac{BC - 2A\pi \omega}{AC + 2B\pi \omega}\right)}{2\pi \omega}.$$

We can use the formulas for the coefficients A, B and C in the two cases to find the lags.

Acknowledgements

References

Abbott, K.D., Ksiazek, T.G., Mills, J.N., 1999. Long-term hantavirus persistence in rodent populations in central Arizona. Emerg. Infect. Dis. 5, 102–112.

Abramson, G., Kenkre, V.M., 2002. Spatiotemporal patterns in the hantavirus infection. Phys. Rev. E 66, 011912.

Allen, L.J.S., McCormack, R.K., Johnson, C.B., 2006. Mathematical models for hantavirus infection in rodents. Bull. Math. Biol. 68, 511–524.

Anderson, R., May, R., 1992. Infectious Diseases of Humans. Oxford University Press, Oxford.

Barlow, N.D., 2000. Non-linear transmission and simple models for bovine tuberculosis. J. Animal Ecol. 69, 703–713.

Begon, M., Feore, S.M., Brown, K., Chantrey, J., Jones, T., Bennett, M., 1998. Population and transmission dynamics of cowpox in bank voles: testing fundamental assumptions. Ecol. Lett. 1, 82–86.

Biggs, J.R., Bennett, K.D., Mullen, M.A., Haarmann, T.K., Salisbury, M., Robinson, R.J., Keller, D., Torrez-Martinez, N., Hjelle, B., 2000. Relationship of ecological variables to Sin Nombre virus antibody seroprevalence in populations of deer mice. J. Mammal. 81, 676–682.

Boone, J.D., Otteson, E.W., McGwire, K.C., Villard, P., Rowe, J.E., Jeor, S.C.S., 1998. Ecology and demographics of hantavirus infections in rodent populations in the Walker River Basin of Nevada and California. Am. J. Trop. Med. Hyg. 59, 445–451.

Botten, J., Mirowsky, K., Ye, C.Y., Gottlieb, K., Saavedra, M., Ponce, L., Hjelle, B., 2002. Shedding and intracage transmission of Sin Nombre hantavirus in the deer mouse (*Peromyscus maniculatus*) model. J. Virol. 76, 7587–7594.

Brown, J.H., Ernest, S.K.M., 2002. Rain and rodents: complex dynamics of desert consumers. Bioscience 52, 979–987.

Buceta, J., Escudero, C., de la Rubia, F.J., Lindenberg, K., 2004. Outbreaks of hantavirus induced by seasonality. Phys. Rev. E 69, 021906.

Caley, P., Ramsey, D., 2001. Estimating disease transmission in wildlife, with emphasis on leptospirosis and bovine tuberculosis in possums, and effects of fertility control. J. Appl. Ecol. 38, 1362–1370.

Calisher, C.H., Sweeney, W., Mills, J.N., Beaty, B.J., 1999. Natural history of Sin Nombre virus in western Colorado. Emerg. Infect. Dis. 5, 126–134.

Calisher, C.H., Mills, J.N., Sweeney, W.P., Choate, J.R., Sharp, D.E., Canestorp, K.M., Beaty, B.J., 2001. Do unusual site-specific population dynamics of rodent reservoirs provide clues to the natural history of hantaviruses? J. Wild. Dis. 37, 280–288.

Calisher, C.H., Root, J.J., Mills, J.N., Rowe, J.E., Reeder, S.A., Jentes, E.S., Wagoner, K., Beaty, B.J., 2005. Epizootiology of Sin Nombre and El Moro Canyon hantavirus, southeastern Colorado, 1995–2000. J. Wild. Dis. 41, 1–11.

Davis, S., Begon, M., De Bruyn, L., Ageyev, V.S., Klassovskiy, N.L., Pole, S.B., Viljugrein, H., Stenseth, N.C., Leirs, H., 2004. Predictive thresholds for plague in Kazakhstan. Science 304, 736–738.

Davis, S., Calvet, E., Leirs, H., 2005. Fluctuating rodent populations and risk to humans from rodent-borne zoonoses. Vector-Borne Zoonotic Dis. 5, 305–314.

Douglass, R.J., Wilson, T., Semmens, W.J., Zanto, S.N., Bond, C.W., Horn, R.C.V., Mills, J.N., 2001. Longitudinal studies of Sin Nombre virus in deer mouse-dominated ecosystems of Montana. Am. J. Trop. Med. Hyg. 65, 33–41.

Engelthaler, D.M., Mosley, D.G., Cheek, J.E., Levy, C.E., Komatsu, K.K., Ettestad, P., Davis, T., Tanda, D.T., Miller, L., Frampton, J.W., Porter, R., Bryan, R.T., 1999. Climatic and environmental patterns associated with hantavirus pulmonary syndrome, Four Corners region, United States. Emerg. Infect. Dis. 5, 87–94.

Enscore, R.E., Biggerstaff, B.J., Brown, T.L., Fulgham, R.F., Reynolds, P.J., Engelthaler, D.M., Levy, C.E., Parmenter, R.R., Montenieri, J.A., Cheek, J.E., Grinnell, R.K., Ettestad, P.J., Gage, K.L., 2002. Modeling relationships between climate and the frequency of human plague cases in the southwestern United States, 1960–1997. Am. J. Trop. Med. Hyg. 66, 186–196.

Escutenaire, S., Chalon, P., Verhagen, R., Heyman, P., Thomas, I., Karelle-Bui, L., Avsic-Zupanc, T., Lundkvist, A., Plyusnin, A., Pastoret, P.P., 2000. Spatial and temporal dynamics of Puumala hantavirus infection in red bank vole (*Clethrionomys glareolus*) populations in Belgium. Virus Res. 67, 91–107.

Fairbairn, D.J., 1977. The spring decline in deer mice: death or dispersal. Can. J. Zool. 55, 84–92.

Glass, G.E., Cheek, J.E., Patz, J.A., Shields, T.M., Doyle, T.J., Thoroughman, D.A., Hunt, D.K., Enscore, R.E., Gage, K.L., Irland, C., Peters, C.J., Bryan, R., 2000. Using remotely sensed data to identify areas at risk for hantavirus pulmonary syndrome. Emerg. Infect. Dis. 6, 238–247.

Graham, T.B., Chomel, B.B., 1997. Population dynamics of the deer mouse (*Peromyscus maniculatus*) and Sin Nombre Virus, California Channel Islands. Emerg. Infect. Dis. 3, 367–370.

Helle, B., Yates, T., (2001) Modeling hantavirus maintenance and transmission in rodent communities. In: Schmaljohn, C.S., Nichol, S.T. (Eds.), Hantaviruses, pp. 77–90. Springer, Berlin.

Hjelle, B., Glass, G.E., 2000. Outbreak of hantavirus infection in the Four Corners region of the United States in the wake of the 1997–1998 El Nino-southern oscillation. J. Infect. Dis. 181, 1569–1573.

Keesing, F., Holt, R.D., Ostfeld, R.S., 2006. Effects of species diversity on disease risk. Ecol. Lett. 9, 485–498.

Kolivras, K.N., Comrie, A.C., 2004. Climate and infectious disease in the southwestern United States. Prog. Phys. Geogr. 28, 387–398.

Kuenzi, A.J., Douglass, R.J., Bond, C.W., Calisher, C.H., Mills, J.N., 2005. Long-term dynamics of Sin Nombre viral RNA and antibody in deer mice in Montana. J. Wildl. Dis. 41, 473–481.

McCallum, H., Barlow, N.D., Hone, J., 2001. How should pathogen transmission be modelled? Trends Ecol. Evol. 16, 295–300.

Mills, J.N., Ksiazek, T.G., Mills, J.N., Ksiazek, T.G., Ellis, B.A., Rollin, P.E., Nichol, S.T., Yates, T.L., Gannon, W.L., Levy, C.E., Engelthaler, D.M., Davis, T., Tanda, D.T., Frampton, J.W., Nichols, C.R., Peters, C.J., Childs, J.E., 1997. Patterns of association with host and habitat: antibody reactive with Sin Nombre virus in small mammals in the major biotic communities of the southwestern United States. Am. J. Trop. Med. Hyg. 56, 273–284.

Mills, J.N., Ksiazek, T.G., Peters, C.J., Childs, J.E., 1999. Long-term studies of hantavirus reservoir populations in the southwestern United States: a synthesis. Emerg. Infect. Dis. 5, 135–142.

Olsson, G.E., White, N., Ahlm, C., Elgh, F., Verlemyr, A.C., Juto, P., Palo, R.T., 2002. Demographic factors associated with hantavirus infection in bank voles (*Clethrionomys glareolus*). Emerg. Infect. Dis. 8, 924–929.

Olsson, G.E., Ahim, C., Elgh, F., Verlemyr, A.C., White, N., Juto, P., Palo, R.T., 2003. Hantavirus antibody occurrence in bank voles (*Clethrionomys glareolus*) during a vole population cycle. J. Wild. Dis. 39, 299–305.

Petticrew, B., Sadleir, R., 1974. The ecology of the deer mouse *Peromyscus maniculatus* in a coastal coniferous forest: population dynamics. Can. J. Zool. 52, 107–118.

R Development Core Team, 2005. R: A language and environment for statistical computing. R Foundation for Statistical Computing, Vienna, Austria. ISBN 3-900051-07-0.

Ramsey, D., Spencer, N., Caley, P., Efford, M., Hansen, K., Lam, M., Cooper, D., 2002. The effects of reducing population density on contact rates between brushtail possums: implications for transmission of bovine tuberculosis. J. Appl. Ecol. 39, 806–818.

Root, J.J., Calisher, C.H., Beaty, B.J., 1999. Relationships of deer mouse movement, vegetative structure, and prevalence of infection with Sin Nombre Virus. J. Wildl. Dis. 35, 311–316.

Root, J.J., Black, W.I.V., Calisher, C.H., Wilson, K.R., Mackie, R.S., Schountz, T., Mills, J.N., Beaty, B.J., 2003. Analyses of gene flow among populations of deer mice (*Peromyscus maniculatus*) at sites near hantavirus pulmonary syndrome case-patient residences. J. Wildl. Dis. 39, 287–298.

Sanchez, A.J., Abbott, K.D., Nichol, S.T., 2001. Genetic identification and characterization of limestone canyon virus, a unique Peromyscus-borne hantavirus. Virol. 286, 345–353.

Sauvage, F., Langlais, M., Pontier, D., 2007. Predicting the emergence of human hantavirus disease using a combination of viral dynamics and rodent demographic patterns. Epidemiol. Infect. 135, 46–56.

Sauvage, F., Langlais, M., Yoccoz, N.G., Pontier, D., 2003. Modelling hantavirus in fluctuating populations of bank voles: the role of indirect transmission on virus persistence. J. Animal Ecol. 72, 1–13.

Schmaljohn, C., Hjelle, B., 1997. Hantaviruses: a global disease problem. Emerg. Infect. Dis. 3, 95–104.

Wolff, J.O., 1985. The effects of density, food, and interspecific interference on home range size in Peromyscus leucopus and Peromyscus maniculatus. Can. J. Zool. 63, 2657–2662.

Yates, T.L., Mills, J.N., Parmenter, C.A., Ksiazek, T.G., Parmenter, R.R., Castle, J.R.V., Calisher, C.H., Nichol, S.T., Abbott, K.D., Young, J.C., Morrison, M.L., Beaty, B.J., Dunnum, J.L., Baker, R.J., Salazar-Bravo, J., Peters, C.J., 2002. The ecology and evolutionary history of an emergent disease: hantavirus pulmonary syndrome. Bioscience 52, 989–998.